11

Control of Induction Machine Drives

Daniel Logue
University of Illinois at Urbana-Champaign

Philip T. Krein
University of Illinois at Urbana-Champaign

11.1 Introduction

Induction machines have become the staple for electromechanical energy conversion in today's industry; they are used more often than all other types of motors combined. Several factors have made them the machine of choice for industrial applications vs. DC machines, including their ruggedness, reliability, and low maintenance [1, 2]. The cage-induction machine is simple to manufacture, with no rotor windings or commutator for external rotor connection. There are no brushes to replace because of wear, and no brush arcing to prevent the machine from being used in volatile environments. The induction machine has a higher power density, greater maximum speed, and lower rotor inertia than the DC machine.

The induction machine has one significant disadvantage with regard to torque control as compared with the DC machine. The torque production of a given machine is related to the cross-product of the stator and rotor flux-linkage vectors [3–5]. If the rotor and stator flux linkages are held orthogonal to one another, the electrical torque of the machine can be controlled by adjusting either the rotor or stator flux-linkage and holding the other constant. The field and armature windings in a DC machine are held orthogonal by a mechanical commutator, making torque control relatively simple. With an induction machine, the stator and rotor windings are not fixed orthogonal to one another. The induction machine is singly excited, with the rotor field induced by the stator field, further complicating torque control. Until a few years ago, the induction machine was mainly used for constant-speed applications. With recent improvements in semiconductor technology and power electronics, the induction machine is seeing wider use in variable-speed applications [6].

This chapter discusses how these challenges related to the induction machine are overcome to effect torque and speed control comparable with that of the DC machine. The first section involves what is termed volts-per-hertz, or scalar, control. This control method is derived from the steady-state machine model and is satisfactory for many low-performance industrial and commercial applications. The rest of the chapter will present vector-controlled methods applied to the induction machine [7]. These methods are aimed at bringing about independent control of the machine torque- and flux-producing stator currents. Developed using the dynamic machine model, vector-controlled induction machines exhibit far better dynamic performance than those with scalar control [8].

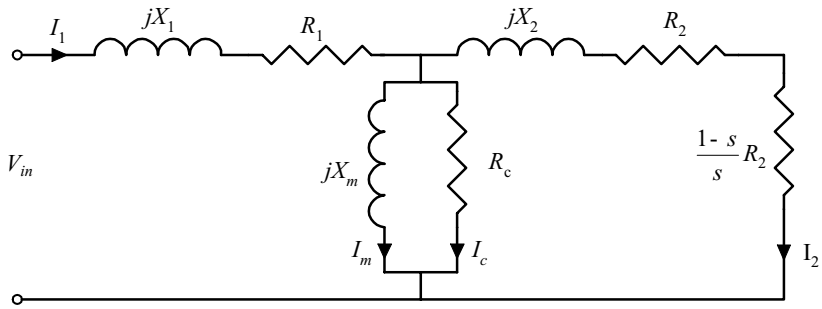

FIGURE 11.1 Induction machine steady-state model.

11.2 Scalar Induction Machine Control

Induction machine scalar control is derived using the induction machine steady-state model shown in Fig. 11.1 [1]. The phasor form of the machine voltages and currents is indicated by capital letters. The stator series resistance and leakage reactance are R_1 and X_1, respectively. The referred rotor series resistance and leakage reactance are R_2 and X_2, respectively. The magnetizing reactance is X_m; the core loss due to eddy currents and the hysteresis of the iron core is represented by the shunt resistance R_c. The machine slip s is defined as [1]

$$s = \frac{\omega_e - \omega_r}{\omega_e} \tag{11.1}$$

where ω_e is the synchronous, or excitation frequency, and ω_r is the machine shaft speed, both in electrical radians-per-second. The power supplied to the machine shaft can be expressed as

$$P_{\text{shaft}} = \frac{1-s}{s} R_2 i_2^2 \tag{11.2}$$

Solving for I_2 and using Eq. (11.2), the shaft torque can be expressed as

$$T_e = \frac{3|V_{\text{in}}|^2 R_2 s}{\omega_e[(sR_1 + R_2)^2 + s^2(X_1 + X_2)^2]} \tag{11.3}$$

where the numeral 3 in the numerator is used to include the torque from all three phases. This expression makes clear that induction machine torque control is possible by varying the magnitude of the applied stator voltage. The normalized torque vs. slip curves for a typical induction machine corresponding to various stator voltage magnitudes are shown in Fig. 11.2. Speed control is accomplished by adjusting the input voltage until the machine torque for a given slip matches the load torque. However, the developed torque decreases as the square of the input voltage, but the rotor current decreases linearly with the input voltage. This operation is inefficient and requires that the load torque decrease with decreasing machine speed to prevent overheating [1, 2]. In addition, the breakdown torque of the machine decreases as the square of the input voltage. Fans and pumps are appropriate loads for this type of speed control because the torque required to drive them varies linearly or quadratically with their speed.

Linearization of Eq. (11.3) with respect to machine slip yields

$$T_e = \frac{3|V_{\text{in}}|^2 s}{\omega_e R_2} = \frac{3|V_{\text{in}}|^2(\omega_e - \omega_r)}{\omega_e^2 R_2} \tag{11.4}$$

The characteristic torque curve can be shifted along the speed axis by changing ω_e with the capability

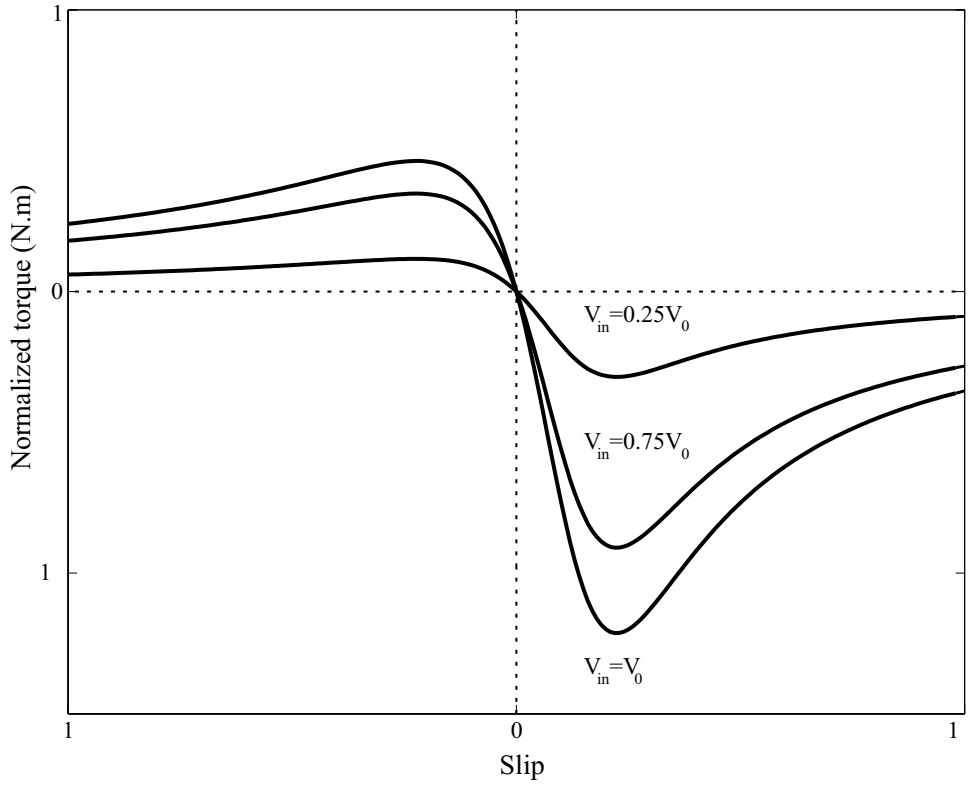

FIGURE 11.2 Normalized torque–slip curves with varying input voltage magnitudes for a typical induction machine.

for developing rated torque throughout the entire speed range given a constant stator voltage magnitude. An inverter is needed to drive the induction machine to implement frequency control.

One remaining complication is the fact that the magnetizing reactance changes linearly with excitation frequency. Therefore, with constant input voltage, the input current increases as the input frequency decreases. In addition, the stator flux magnitude increases as well, possibly saturating the machine. To prevent this from happening, the input voltage must be varied in proportion to the excitation frequency. From Eq. (11.4), if the input voltage and frequency are proportional with proportionality constant k_f, the electrical torque developed by the machine can be expressed as

$$T_e = \frac{3k_f^2}{R_2}(\omega_e - \omega_r) \tag{11.5}$$

and demonstrates that the torque response of the machine is uniform throughout the full speed range.

The block diagram for the scalar-controlled induction drive is shown in Fig. 11.3. The inverter DC-link voltage is obtained through rectification of the AC line voltage. The drive uses a simple pulse-width-modulated (PWM) inverter whose time-average output voltages follow a reference-balanced three-phase set, the frequency and amplitude of which are provided by the speed controller. The drive shown here uses an active speed controller based on a proportional integral derivative (PID), or other type of controller. The input to the speed controller is the error between a user-specified reference speed and the shaft speed of the machine. An encoder or other speed-sensing device is required to ascertain the shaft speed. The drive can be operated in the open-loop configuration as well; however, the speed accuracy will be reduced significantly.

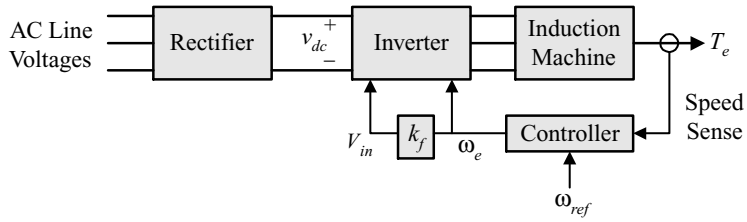

FIGURE 11.3 Block diagram of scalar induction machine drive.

Practical scalar-controlled drives have additional functionality, some of which is added for the convenience of the user. In a practical drive, the relationship between the input voltage magnitude and frequency takes the form

$$|V_{\text{in}}| = k_f \omega_e + V_{\text{offset}} \tag{11.6}$$

where V_{offset} is a constant. The purpose of this offset voltage is to overcome the voltage drop created by the stator series resistance. The relationship (11.6) is usually a piecewise linear function with several breakpoints in a standard scalar-controlled drive. This allows the user to tailor the drive response characteristic to a given application.

11.3 Vector Control of Induction Machines

The derivation of the vector-controlled (VC) method and its application to the induction machine is considered in this section. The vector description of the machine will be derived in the first subsection, followed by the dynamic model description in the second subsection. Field-oriented control (FOC) of the induction machine will be presented in the third subsection and the direct torque control (DTC) method will be described in the last subsection.

Vector Formulation of the Induction Machine

The stator and rotor windings for the three-phase induction machine are shown in Fig. 11.4 [3]. The windings are sinusoidally distributed, but are indicated on the figure as point windings. If N_0 is the number of turns for each winding, then the winding density distributions as functions of θ are given by

$$\begin{aligned} N_a(\theta) &= N_0 \cos(\theta) \\ N_b(\theta) &= N_0 \cos\left(\theta - \frac{2\pi}{3}\right) \\ N_c(\theta) &= N_0 \cos\left(\theta + \frac{2\pi}{3}\right) \end{aligned} \tag{11.7}$$

where θ is the angle around the stator referenced from phase *as*-axis. The magnemotive force (MMF) distributions corresponding to (11.7) are [5]

$$\begin{aligned} F_{as}(t, \theta) &= \frac{N_0}{2} i_{as}(t) \cos(\theta) \\ F_{bs}(t, \theta) &= \frac{N_0}{2} i_{bs}(t) \cos\left(\theta - \frac{2\pi}{3}\right) \\ F_{cs}(t, \theta) &= \frac{N_0}{2} i_{cs}(t) \cos\left(\theta + \frac{2\pi}{3}\right) \end{aligned} \tag{11.8}$$

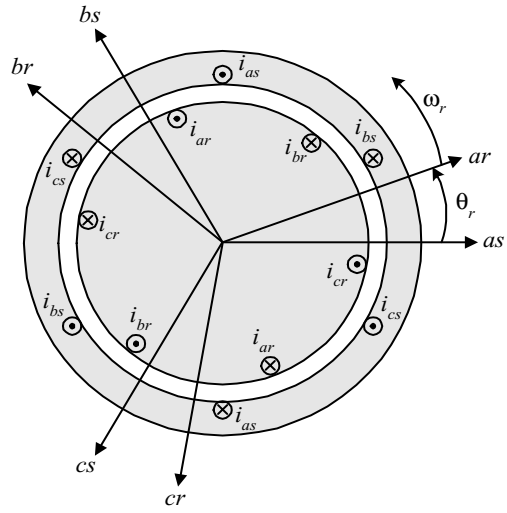

FIGURE 11.4 Induction machine stator and rotor windings.

These scalar equations can be represented by dot products between the following MMF vectors

$$\begin{aligned}
\vec{F}_{as}(t) &= \frac{N_0}{2}\, i_{as}(t)\hat{e}_{as} \\
\vec{F}_{bs}(t) &= \frac{N_0}{2}\, i_{bs}(t)\, \hat{e}_{bs} \\
\vec{F}_{cs}(t) &= \frac{N_0}{2}\, i_{cs}(t)\hat{e}_{cs}
\end{aligned} \tag{11.9}$$

and the unit vector whose angle with the *as*-axis is θ. The vectors $\hat{e}_{as}$, $\hat{e}_{bs}$, and $\hat{e}_{cs}$ represent unit vectors along the respective winding axes. All the machine quantities, including the phase currents and voltages, and flux linkages can be expressed in this vector form.

The vectors along the three axes *as*, *bs*, and *cs* do not form an independent basis set. It is convenient to transform this basis set to one that is orthogonal, the so-called *dq*-transformation, originally proposed by R. H. Park for application to the synchronous machine [3, 9]. Figure 11.5 illustrates the relationship between the degenerate *abc* and orthogonal *qd*0 vector sets. If ϕ is the angle between i_{qs} and i_{as}, then the transformation relating the two coordinate systems can be expressed as

$$\mathbf{i}_{qd0s} = \mathbf{W}(\phi)\mathbf{i}_{abcs} = \frac{2}{3}\begin{bmatrix} \cos\phi & \cos\left(\phi - \frac{2\pi}{3}\right) & \cos\left(\phi + \frac{2\pi}{3}\right) \\ \sin\phi & \sin\left(\phi - \frac{2\pi}{3}\right) & \sin\left(\phi + \frac{2\pi}{3}\right) \\ \frac{1}{2} & \frac{1}{2} & \frac{1}{2} \end{bmatrix}\mathbf{i}_{abcs} \tag{11.10}$$

where $\mathbf{i}_{qd0s} = [i_{qs}\ \ i_{ds}\ \ i_{0s}]^T$ and $\mathbf{i}_{abcs} = [i_{as}\ \ i_{bs}\ \ i_{cs}]^T$. The variable i_{0s} is called the zero-sequence component and is obtained using the last row in the matrix $\mathbf{W}$ [3]. This last row is included to make the matrix invertible, providing a one-to-one transformation between the two coordinate systems. This row is not needed if the transformation acts on a balance set of variables, because the zero-sequence component is

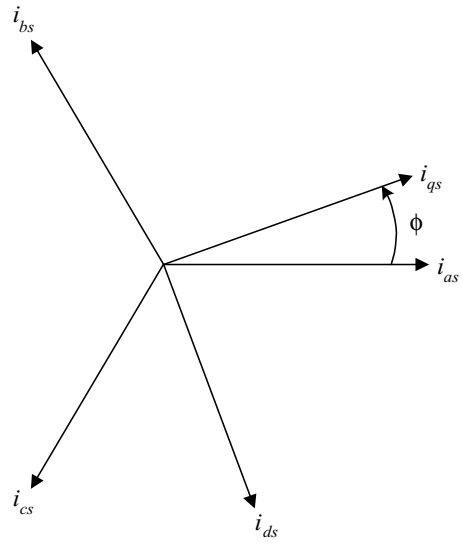

FIGURE 11.5 Illustration for reference frame transformation.

equal to zero. The zero-sequence component carries information about the neutral point of the *abc* variables being transformed. If the set is not balanced, this neutral point is not necessarily zero.

The constant multiplying the matrix of (11.10) is, in general, arbitrary. With this constant equal to $\frac{2}{3}$ as it is in (11.10), the result is the power invariant transformation. By using this transformation, the calculated power in the *abc* coordinate system is equal to that computed in the *qd*0 system [3].

If the angle $\phi = 0$, the result is a transformation from the stationary *abc* system to the stationary *qd*0 system. However, transformation to a reference frame rotating at an arbitrary speed ω is possible by defining

$$\phi(t) = \int_0^t \omega \, d\tau \tag{11.11}$$

As will be seen later, the rotor flux–oriented vector control method makes use of this concept, transforming the machine variables to the synchronous reference frame where they are constants in steady state [4].

To understand this concept intuitively, consider the balanced set of stator MMF vectors of a typical induction machine given in (11.9). It is not difficult to show that the sum of these vectors produces a resultant MMF vector that rotates at the frequency of the stator currents. The length of the vector is dependent upon the magnitude of the MMF vectors. Observing the system from the synchronous reference frame effectively removes the rotational motion, resulting in only the magnitude of the vector being of consequence. If the magnitudes of the MMF vectors are constant, then the synchronous variables will be constant. Transients in the magnitudes of the stationary variables result in transients in the synchronous variables. This is true for currents, voltages, and other variables associated with the machine.

Induction Machine Dynamic Model

The six-state induction machine model in the arbitrary reference frame is presented in this section. This dynamic model will be used to derive the FOC and DTC methods. As will be seen, the derivations of these control methods will be simpler if they are performed in a specific coordinate reference frame. An additional advantage is that transforming to the *qd*0 coordinate system in any reference frame removes

TABLE 11.1 Induction Machine Nomenclature

Induction Machine Parameter or Variable	Symbol
Stator voltages (V)	v_{qs}, v_{ds}
Stator currents (A)	i_{qs}, i_{ds}
Stator flux-linkages (Wb)	λ_{qs}, λ_{ds}
Rotor voltages (V)	v_{qr}, v_{dr}
Rotor currents (A)	i_{qr}, i_{dr}
Rotor flux-linkages (Wb)	λ_{qr}, λ_{dr}
Reference frame speed (rad/s)	ω
Rotor speed (rad/s)	ω_r
Stator series resistance (Ω)	r_s
Stator leakage inductance (H)	L_{ls}
Rotor series resistance (Ω)	r_r
Rotor leakage inductance (H)	L_{lr}
Magnetizing inductance (H)	L_m
Number of machine poles	P
Developed electrical torque (N·m)	T_e
Machine load torque (N·m)	T_{load}
Torque due to windage and friction losses (N·m)	T_{loss}

the time-varying inductances associated with the induction machine [10]. The machine model in a given reference frame is obtained by substituting the appropriate frequency for ω in the model equations.

The state equations for the six-state induction motor model in the arbitrary reference frame are given in Eqs. (11.12) through (11.22) [3, 4]. The induction machine nomenclature is provided in Table 11.1. The derivative operator is denoted by p, and the rotor quantities are referred to the stator. The state equations are

$$v_{qs} = r_s i_{qs} + p\lambda_{qs} + \omega\lambda_{ds} \tag{11.12}$$

$$v_{ds} = r_s i_{ds} + p\lambda_{ds} - \omega\lambda_{qs} \tag{11.13}$$

$$v_{qr} = 0 = r_r i_{qr} + p\lambda_{qr} + (\omega - \omega_r)\lambda_{dr} \tag{11.14}$$

$$v_{dr} = 0 = r_r i_{dr} + p\lambda_{dr} - (\omega - \omega_r)\lambda_{qr} \tag{11.15}$$

$$p\omega_r = \frac{P}{2J}(T_e - T_{\text{load}} - T_{\text{loss}}) \tag{11.16}$$

$$p\theta_r = \omega_r \tag{11.17}$$

where the stator and rotor flux linkages are given by

$$\lambda_{ds} = L_{ls} i_{ds} + L_m(i_{ds} + i_{dr}) \tag{11.18}$$

$$\lambda_{qs} = L_{ls} i_{qs} + L_m(i_{qs} + i_{qr}) \tag{11.19}$$

$$\lambda_{dr} = L_{lr} i_{dr} + L_m(i_{ds} + i_{dr}) \tag{11.20}$$

$$\lambda_{qr} = L_{lr} i_{qr} + L_m(i_{qs} + i_{qr}) \tag{11.21}$$

The electrical torque developed by the machine is [4, 5]

$$T_e = \frac{3PL_m}{4L_r}(\lambda_{dr}i_{qs} - \lambda_{qr}i_{ds}) = \frac{3PL_m}{L_rL'_s}(\lambda_{qs}\lambda_{dr} - \lambda_{qr}\lambda_{ds}) \tag{11.22}$$

where the stator transient reactance is defined as $L'_s = L_s - L_m^2/L_r$, where $L_r = L_{lr} + L_m$ and $L_s = L_{ls} + L_m$. It is important to note that in Eqs. (11.14) and (11.15), the shaft speed ω_r is expressed in electrical radians-per-second, that is, scaled by the number of machine pole pairs.

Field-Oriented Control of the Induction Machine

Field-oriented control is probably the most common control method used for high-performance induction machine applications. Rotor flux orientation (RFO) in the synchronous reference frame is considered here [4]. There are other orientation possibilities, but rotor flux orientation is the most prominent, and so will be presented in detail.

The RFO control method involves making the induction machine behave similarly to a DC machine. The rotor flux is aligned entirely along the *d*-axis. The stator currents are split into two components: a field-producing component that induces the rotor flux and a torque-producing component that is orthogonal to the rotor field. This is analogous to the DC machine where the field flux is along one direction, and the commutator ensures an orthogonal armature current vector. This task is greatly simplified through transformation of the machine variables to the synchronously rotating reference frame.

Under FOC, the *q*-axis rotor flux linkage is zero in the synchronous reference frame, by using Eq. (11.22), the electric torque of the induction machine can be expressed as

$$T_e = \frac{3PL_m}{4L_r}\lambda^e_{dr}i^e_{qs} \tag{11.23}$$

where the *e* superscript indicates evaluation in the synchronous reference frame. This torque equation is very similar to that of the DC machine. If either the flux linkage λ^e_{dr} or current i^e_{qs} is held constant, then the torque can be controlled by changing the other. Assuming the inverter driving the induction machine is current sourced, the stator currents can be controlled almost instantaneously. However, by setting $\lambda^e_{qr} = 0$ in Eq. (11.15) and substituting the result in Eq. (11.20), it can be shown that the *d*-axis rotor flux linkage is governed by

$$\lambda^e_{dr} = \frac{L_m r_r}{(L_{lr} + L_m)p + 1} i^e_{ds} = \frac{L_m}{\tau_r p + 1} i^e_{ds} \tag{11.24}$$

where τ_r is termed the rotor time constant. Equation (11.24) dictates that the rotor flux cannot be changed arbitrarily fast. Therefore, the best dynamic torque response will result if the rotor flux linkage is held constant, and the electrical torque is controlled by changing i^e_{qs}. Assuming a current-sourced inverter, this control configuration allows torque control for which the response is limited only by the response time of the inverter driving the machine.

Implementation of RFO control requires that the machine variables be transformed to the synchronous reference frame. To accomplish this task, the synchronous reference frame speed must be calculated in some manner. There are two common methods of finding the synchronous speed. In indirect FOC, the synchronous speed is obtained by using a rotor speed measurement and a corresponding slip calculation [4, 11]. Direct FOC uses air-gap flux measurement or other machine-related quantities to compute the synchronous speed. The indirect method is the most common and will be presented here.

In indirect FOC, the synchronous reference frame speed must be found, and this value integrated to obtain the angle used in the reference frame transformation $W(\phi)$. Rewriting Eq. (11.14) with $\lambda_{qr}^{e} = 0$ yields

$$\omega_e - \omega_r = -\frac{\lambda_{dr}^{e}}{r_r i_{qr}^{e}} \tag{11.25}$$

Again, with $\lambda_{qr}^{e} = 0$, rewrite Eq. (11.21) as

$$i_{qr}^{e} = -\frac{L_m i_{qs}^{e}}{L_{lr} + L_m} \tag{11.26}$$

Substitution of Eq. (11.26) into Eq. (11.25) yields the desired expression for ω_e

$$\omega_e = \omega_r + \frac{(L_{lr} + L_m)\lambda_{dr}^{e}}{L_m r_r i_{qs}^{e}} = \omega_r + \frac{\tau_r}{L_m}\frac{\lambda_{dr}^{e}}{i_{qs}^{e}} \tag{11.27}$$

This expression provides the needed synchronous speed in terms of the rotor flux, which is specified by the controller, and the q-axis stator current that is adjusted for torque control. The rotor flux time constant τ_r is required for the slip calculation, and in many cases must be estimated online because of its dependence on temperature and other factors [12, 13]. The d-axis stator current needed to produce a given rotor flux can be computed using Eq. (11.24). The angle ϕ used for the reference frame transformation is calculated via

$$\phi(t) = \int_0^t \omega_e \, d\tau + \phi(0) \tag{11.28}$$

The block diagram for the FOC drive is shown in Fig. 11.6. The current i_{qs}^{e*} is used for torque control, while the current i_{ds}^{e*} is calculated using the reference rotor flux λ_{dr}^{e*}. Also present in the diagram is an optional speed controller (connected via the dotted lines) that uses the error between a reference value and the actual

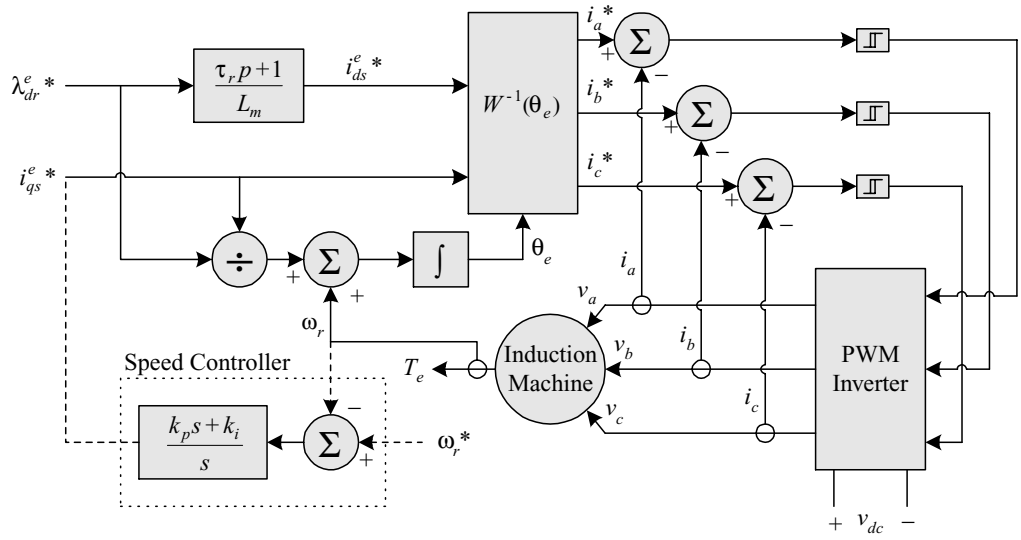

FIGURE 11.6 Block diagram of the indirect FOC drive.

machine speed to control the q-axis stator current. The machine reference currents in the stationary reference frame i_a^*, i_b^*, and i_c^* are computed using the transformation $W^{-1}(\phi)$. The inverter phase voltages are determined using hysteretic controllers [14]. Other methods include ramp comparison and predictive controllers. The shaft speed of the induction machine is obtained using a shaft encoder or similar device.

In the above setup, the inverter voltages were dynamically controlled using the stator current error. The stator voltages required to produce the currents i_a^*, i_b^*, and i_c^*, can also be computed directly using the induction machine model. The stator voltage Eqs. (11.12) and (11.13) must first be "decoupled" to control the armature currents independently. This is because these equations contain stator flux linkage terms that are dependent upon the rotor currents. The decoupling is accomplished by first substituting Eqs. (11.20) and (11.21) into Eqs. (11.18) and (11.19), respectively. The resulting forms of Eqs. (11.18) and (11.19) are then substituted into the stator voltage Eqs. (11.12) and (11.13) to yield [4]

$$v_{qs}^e = (r_s + L_s' p) i_{qs}^e + \omega_e \left(L_s' i_{ds}^e + \frac{L_m}{L_r} \lambda_{dr}^e \right) \tag{11.29}$$

$$v_{ds}^e = (r_s + L_s' p) i_{ds}^e - \omega_e L_s' i_{qs}^e + \frac{L_m}{L_r} p \lambda_{dr}^e \tag{11.30}$$

The decoupled voltage equations allow a voltage-sourced inverter to be used directly for FOC. Note that this is not the only method of performing the decoupling, that PID or other controllers can be used to generate the cross-coupled terms in the voltage equations. However, this technique requires estimation of the torque and rotor flux linkage.

Figures 11.7 and 11.8 display the response of a typical induction machine under FOC. The top plot in Fig. 11.7 shows the machine speed reference (dotted line) and the shaft speed (solid line). Initially, the

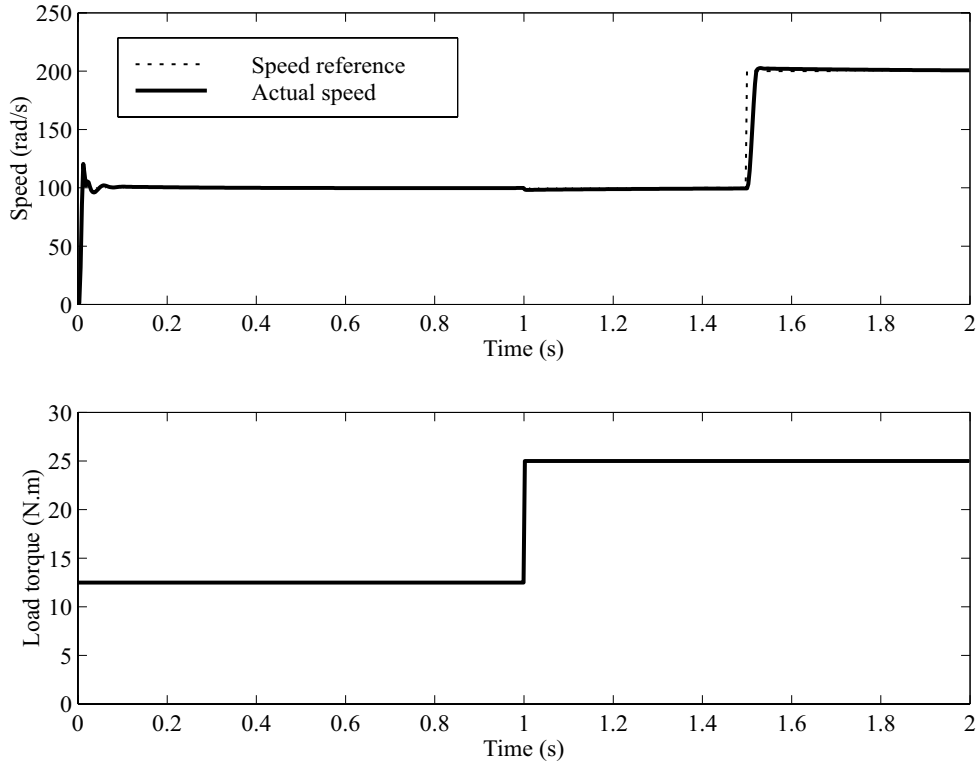

FIGURE 11.7 Induction machine speed reference, actual speed, and load torque.

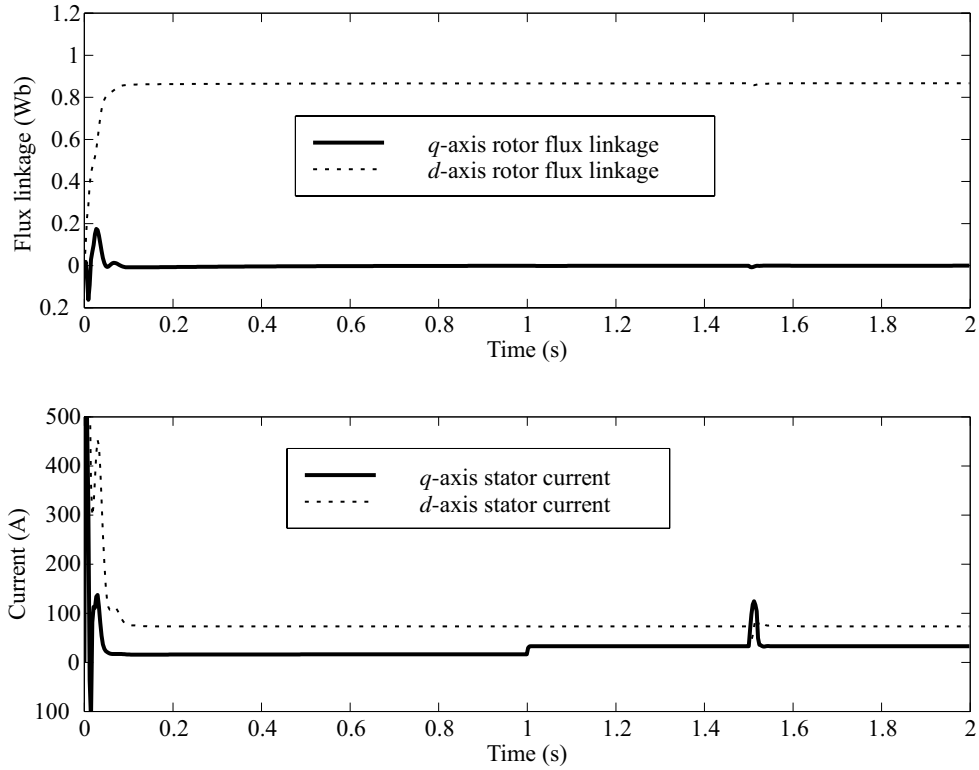

FIGURE 11.8 Rotor flux-linkage and stator currents for the FOC induction machine example.

speed reference is equal to 100 rad/s, and at $t = 1.5$ s, the reference is stepped to 200 rad/s. The machine load is shown in the lower plot. The initial load is 12 N·m and is stepped to 25 N·m at $t = 1$ s. These plots demonstrate that the FOC induction machine has a fast dynamic response and good disturbance rejection.

The rotor dq flux linkages are shown in the top plot of Fig. 11.8. The q-axis flux linkage settles to zero shortly after startup, and the d-axis flux linkage settles to the reference value. This plot verifies that the rotor flux is oriented along one axis in the synchronous reference frame. The synchronous frame stator currents are given in the lower plot of Fig. 11.8. The d-axis current settles to a constant value corresponding the constant rotor flux linkage value. The q-axis current is stepped at $t = 1$ s to satisfy the load torque and experiences a transient at $t = 1.5$ s to increase the machine speed.

Direct Torque Control of the Induction Machine

Whereas the FOC method maintains orthogonality between the rotor flux linkage and the stator torque-producing current, the DTC method directly controls the stator flux linkage to effect torque control [15–18]. The DTC method operates in the stationary reference frame and acts directly on the inverter switches to produce the necessary stator voltages. Hysteretic controllers are used to constrain the electrical torque and stator flux magnitude within certain bounds.

Space Vector Modulation

A DTC drive is constructed using a three-phase switch matrix as shown in Fig. 11.9. The DC input voltage is denoted v_{dc} and the each of the switches has an associated switching function, given by

$$q_{1i} = \begin{cases} 1 & q_{1i} \quad \text{on}, \\ 0 & q_{1i} \quad \text{off}, \end{cases} \qquad i \in [1, 2, 3] \tag{11.31}$$

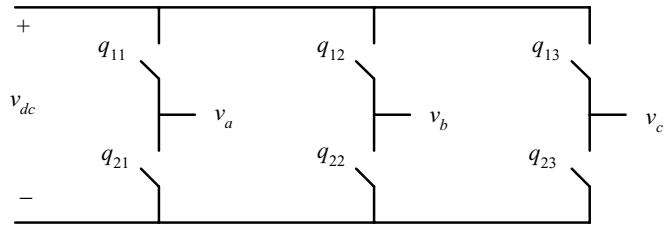

FIGURE 11.9 Switch matrix for the three-phase inverter.

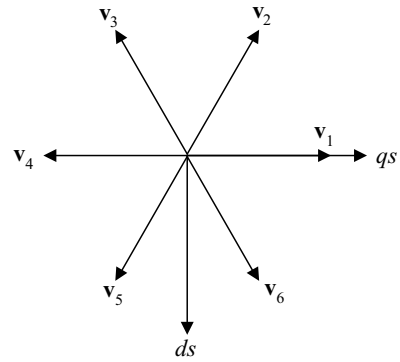

FIGURE 11.10 Voltage star for the three-phase inverter switch matrix.

where $q_{1i} = 1 - q_{2i}$. The result is eight inverter configurations enumerated by $[q_{11}\ \ q_{12}\ \ q_{13}]$. For example, in configuration $[1\ \ 0\ \ 0]$, phase a is connected to the positive side of the DC bus, and phases b and c are connected to the negative side. These eight inverter configurations yield eight equivalent voltage vectors in the $dq0$ coordinate system as displayed in Fig. 11.10.

The diagram in Fig. 11.10 is called the *voltage star* for the three-phase inverter [15]. It is arrived at from the various configurations in Fig. 11.9 and using the transformation (11.10) with $\phi = 0°$. The voltage vector $\mathbf{v}_1$ is calculated using the coordinate transformation and the values $v_a = \frac{2}{3}v_{dc}$ and $v_b = v_c = -\frac{1}{3}v_{dc}$, and is equal to $\mathbf{v}_1 = \frac{2}{3}v_{dc}\hat{e}_q + 0\hat{e}_d$. The set of voltage vectors in polar coordinates provided by the inverter are collectively given by [5, 19]

$$\mathbf{v}_k = \begin{cases} \frac{2}{3}v_{dc}\hat{r}e^{[j(k-1)\pi/3]\hat{\theta}} & k = 1, \ldots, 6 \\ 0 & k = 0, 7 \end{cases} \tag{11.32}$$

where $(\hat{r}, \hat{\theta})$ is the polar coordinate representation of $(\hat{e}_q, \hat{e}_d)$. The vectors $\mathbf{v}_0$ and $\mathbf{v}_7$ correspond to the case where $q_{11} = q_{12} = q_{13} = 0$.

Direct Torque Control Concept

From Eqs. (11.12) and (11.13), the stator flux linkages in the stationary reference frame are computed via [5, 15]

$$\lambda_{qs}^s(t) = \int_0^t (v_{qs}^s(\tau) - r_s i_{qs}^s(\tau))d\tau \tag{11.33}$$

$$\lambda_{ds}^s(t) = \int_0^t (v_{ds}^s(\tau) - r_s i_{ds}^s(\tau))d\tau \tag{11.34}$$

where the superscripted s indicates evaluation in the stationary reference frame. If the stator resistance r_s is small, as is usually the case, the stator flux linkages can be approximated as the time integral of the stator voltages. This approximation coupled with the space vector development above provides the means for directly controlling the stator flux linkage vector by manipulation of the stator voltages.

The electrical torque developed by the three-phase induction machine (11.22) can be written as the cross product [3, 4]

$$T_e = \frac{3PL_m}{4L'_m}\boldsymbol{\lambda}_s^s \times \boldsymbol{\lambda}_r^s = \frac{3PL_m}{4L'_m}\left|\boldsymbol{\lambda}_s^s\right|\left|\boldsymbol{\lambda}_r^s\right|\sin(\rho) \tag{11.35}$$

where $\boldsymbol{\lambda}_s^s = [\lambda_{ds}^s \;\; \lambda_{qs}^s]^T$, $\boldsymbol{\lambda}_r^s = [\lambda_{dr}^s \;\; \lambda_{qr}^s]^T$, and ρ is the angle between the stator and rotor flux linkages. It is clear from Eq. (11.35), if the stator and rotor flux linkage magnitudes are held constant, then the machine torque can be controlled by changing the angle ρ. The angle ρ cannot be changed directly, but can be indirectly modified by changing the stator flux linkage angle rapidly. This is because the stator flux time constant is typically much faster than the rotor flux time constant. If the stator flux linkage is changed quickly, the rotor flux will lag behind, resulting in a change in ρ.

Hysteretic comparators are used to control the inverter switches to adjust the magnitude and angle of the stator flux linkage. This is because the voltages cannot be controlled through continuous ranges, only two discrete levels: each phase can only be connected to either the positive or negative DC bus voltage. The two-level hysteretic control function is defined as

$$g(t, x, \varepsilon, X_0) = \begin{cases} G_1 & x(t) > X_0 + \varepsilon \\ g(t) & X_0 + \varepsilon \geq x(t) \geq X_0 - \varepsilon \\ G_2 & x(t) < X_0 - \varepsilon \end{cases} \tag{11.36}$$

The two quantities to be controlled are the electrical torque via the angle ρ, and the stator flux linkage magnitude. The hysteretic controllers are used to maintain these two quantities within the ranges $\lambda_{\text{ref}} + \Delta\lambda \geq \left|\boldsymbol{\lambda}_s^s\right| \geq \lambda_{\text{ref}} - \Delta\lambda$ and $T_{\text{ref}} + \Delta T \geq T_e \geq T_{\text{ref}} - \Delta T$. The comparators provide the necessary inverter switch configurations to ensure that the torque and stator flux linkage magnitude stay within these limits. A rule set relating the torque and stator flux linkage error to the set of inverter configurations must be developed. To simplify this task, the coordinate frame is separated into sectors as shown in Fig. 11.11. There are six sectors corresponding to the six active inverter states.

To understand why the sectors are used, consider the situation where the stator flux linkage vector is in Sector 1, and its magnitude and angle γ must be increased. If the stator voltage vector $\mathbf{v}_2$ is used, the flux linkage magnitude and the angle γ will both increase no matter where the flux linkage vector resides in Sector 1. The vector $\mathbf{v}_1$ cannot be reliably used to accomplish this goal, because if the stator flux linkage vector is ahead of $\mathbf{v}_1$, the angle γ will decrease, resulting in a torque decrease. All of the appropriate controller responses can be worked out this way to form the lookup table shown in Table 11.2 [4]. Given the sector number in which the stator flux linkage resides and the outputs of the flux linkage magnitude and torque hysteretic comparators, the table provides the required inverter voltage vector. The flux linkage comparator is two level, and the torque comparator is three level. If the estimated torque is within the specified bounds of the comparator, a zero voltage vector is selected. In this case, the zero voltage vector that requires the fewest inverter switches changing state is used.

To implement the control described above, the sector number must be determined. The most straightforward way of accomplishing this is to find the stator flux linkage angle γ trigonometrically:

$$\gamma = \tan^{-1}\left(\frac{\lambda_{sq}^s}{\lambda_{sd}^s}\right) \tag{11.37}$$

TABLE 11.2 Optimum Lookup Table for DTC Inverter Control

$\lvert\boldsymbol{\lambda}_s^s\rvert$	T_e	Sector 1	Sector 2	Sector 3	Sector 4	Sector 5	Sector 6
Increase	Increase	$\mathbf{v}_2$	$\mathbf{v}_3$	$\mathbf{v}_4$	$\mathbf{v}_5$	$\mathbf{v}_6$	$\mathbf{v}_1$
Increase	Within limits	$\mathbf{v}_7$	$\mathbf{v}_0$	$\mathbf{v}_7$	$\mathbf{v}_0$	$\mathbf{v}_7$	$\mathbf{v}_0$
Increase	Decrease	$\mathbf{v}_6$	$\mathbf{v}_1$	$\mathbf{v}_2$	$\mathbf{v}_3$	$\mathbf{v}_4$	$\mathbf{v}_5$
Decrease	Increase	$\mathbf{v}_3$	$\mathbf{v}_4$	$\mathbf{v}_5$	$\mathbf{v}_6$	$\mathbf{v}_1$	$\mathbf{v}_2$
Decrease	Within limits	$\mathbf{v}_0$	$\mathbf{v}_7$	$\mathbf{v}_0$	$\mathbf{v}_7$	$\mathbf{v}_0$	$\mathbf{v}_7$
Decrease	Decrease	$\mathbf{v}_5$	$\mathbf{v}_6$	$\mathbf{v}_1$	$\mathbf{v}_2$	$\mathbf{v}_3$	$\mathbf{v}_4$

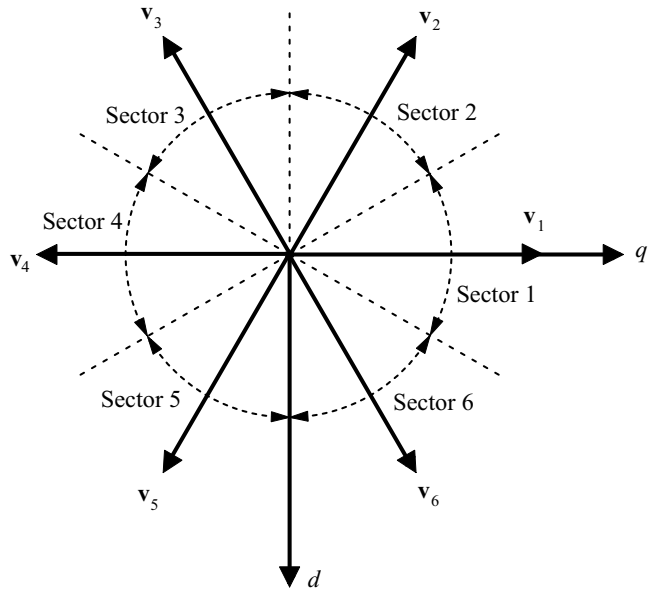

FIGURE 11.11 Sector diagram for the DTC control method.

Given the flux linkage angle, the sector number is easily found. In practice, this method is not used because of the computational burden that the trigonometric inverse places upon the controller. Practical controllers rely on the signs of the flux linkage components to determine the sector number.

One of the major disadvantages of the DTC method is the required accurate estimation of the stator flux linkage and the developed electrical torque. The stator flux linkage is estimated using Eqs. (11.33) and (11.34) with, perhaps, current feedback for correction. The torque is usually estimated using

$$T_e = \frac{3P}{4}\boldsymbol{\lambda}_s^s \times \mathbf{i}_s^s \tag{11.38}$$

There are several variants, but these are the most common ways of performing the estimates. The speed of the estimates must be quite fast, with common values for the sampling time in the neighborhood of 25 μs [15]. If the sampling time is not fast enough, excursion outside the limits imposed by the torque and flux comparators will occur.

The block diagram of the DTC induction machine drive is shown in Fig. 11.12. The error between the reference torque and the estimated torque is fed to a three-level hysteretic comparator, and the speed error is given to a two-level comparator. The outputs of the comparators are supplied to a vector lookup table that makes uses of the relationships in Table 11.2. The optimal switch states are supplied to the PWM inverter that drives the induction machine. The machine torque, stator flux vector, and stator flux sector are estimated online from the machine phase b and c voltages and currents.

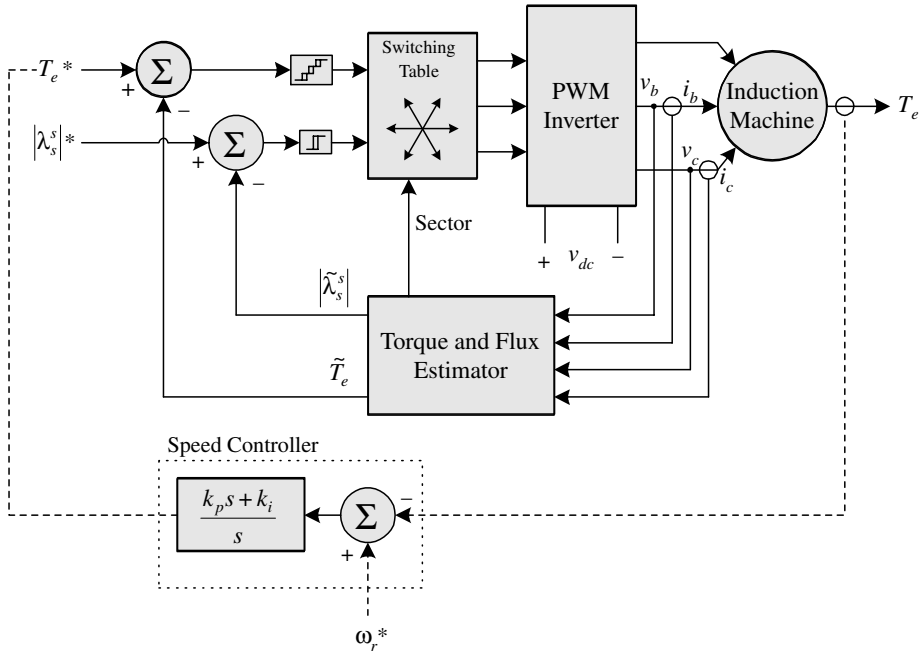

FIGURE 11.12 Block diagram of the DTC induction machine drive.

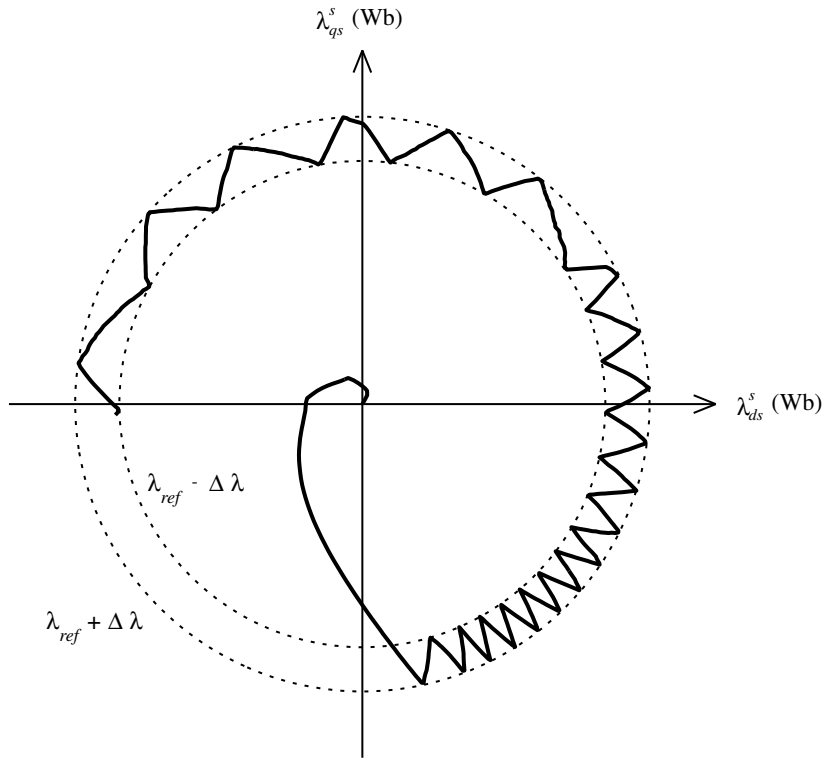

FIGURE 11.13 Stator flux linkage under DTC.

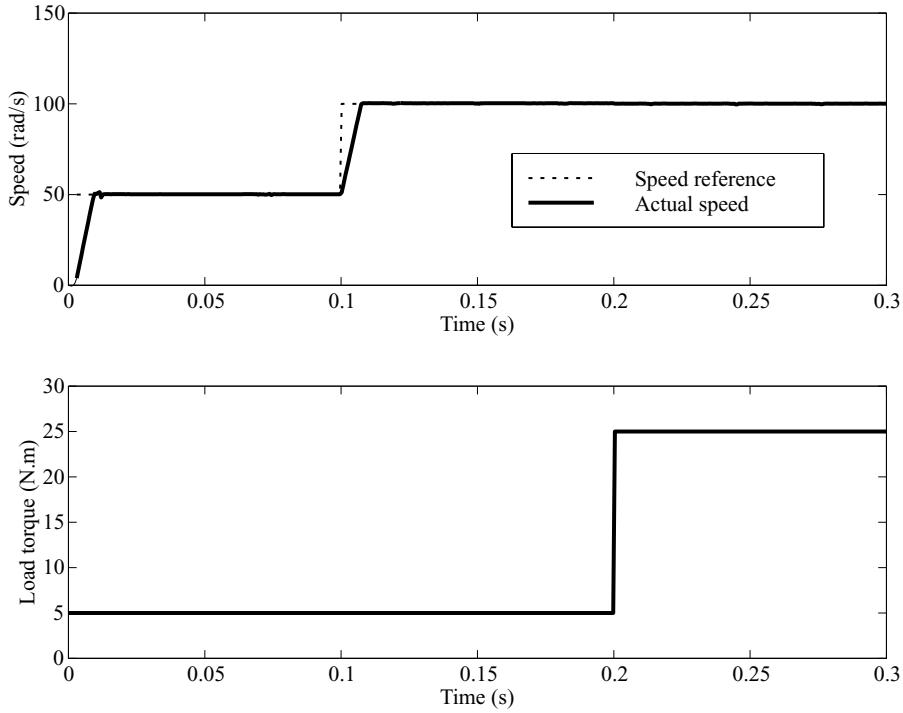

FIGURE 11.14 Speed reference, actual shaft speed, and load torque for the DTC drive example.

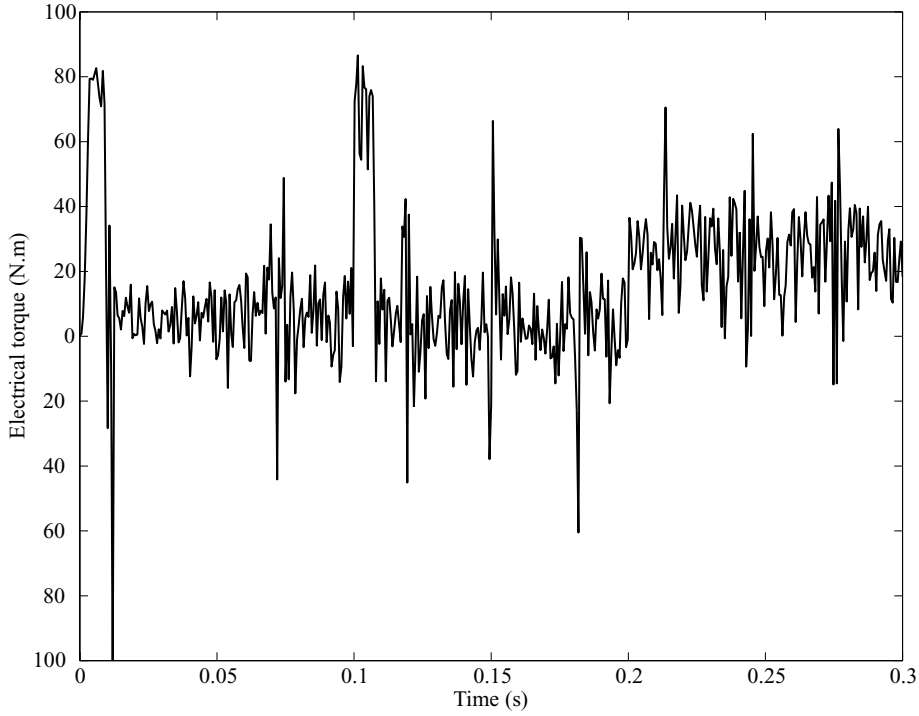

FIGURE 11.15 The electrical torque for the DTC drive.

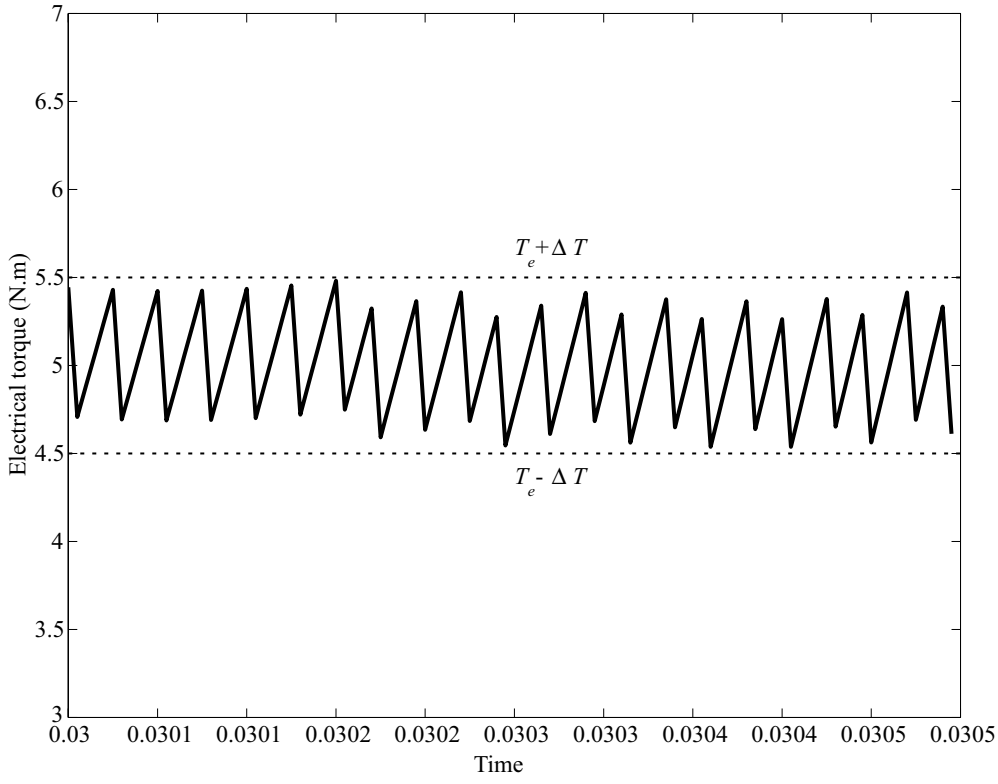

FIGURE 11.16 Electrical torque of the DTC drive.

The stator flux linkage vector is shown in Fig. 11.13 during start-up of a typical DTC drive. The flux linkage limits $\lambda_{ref} \pm \Delta\lambda$ limits of the hysteretic comparator are shown as dashed lines. The flux linkage vector circles the origin with its magnitude confined within these boundaries. The speed of the rotation of the flux linkage vector is determined by the estimated torque error of the machine. Since the machine requires knowledge of the stator flux linkage sector, start-up of the machine is not as simple as for the FOC drive. Typically, the machine is excited with a small DC current to establish the sector number needed for the controller.

An example of the operation of typical DTC drive will now be considered. The reference speed, actual speed, and load torque for the machine are displayed in Fig. 11.14. The initial speed reference is 50 rad/s, and is stepped to 100 rad/s at $t = 0.1$ s. The load torque is initially 5 N·m, and is stepped to 25 N·m at $t = 0.2$ s. Note that the drive has excellent response and disturbance rejection, typically better than that of the RFO controlled drive. The electrical torque as a function of time for the DTC drive is shown in Fig. 11.15. Due to the lower switching frequency of the drive, the torque ripple of the DTC drive is considerably greater than for the FOC drive. A close-up of the torque ripple is shown in Fig. 11.16. The minimum and maximum boundaries of the hysteretic comparator are shown as dashed lines.

11.4 Summary

The evolution of induction machine control began with the development of the scalar-controlled method allowing variable speed control. However, the scalar-controlled induction machine failed to match the dynamic performance of a comparable DC drive. The next step was the introduction of the vector-controlled methods. The goal of these methods is to make the induction machine emulate the DC machine by transforming the stator currents to a specific coordinate system where one coordinate is related to the

torque production and the other to rotor flux. The FOC methods provide excellent dynamic response, matching that of the DC machine. The main disadvantage of such controls is the computational overhead required in the coordinate transformation.

The latest development in induction machine control is the DTC method. DTC does not rely on coordinate transformation, but rather controls the stator flux linkage in the stationary reference frame. Despite its control simplicity, the DTC method provides possibly the best dynamic response of any of the methods. The average switching frequency of the drive is lower as well, reducing switching loss as compared with the FOC drive. Since the control basis is the stator flux linkage, the DTC drive is capable of advanced functions such as performing "flying starts" and flux braking [15, 18]. Its main disadvantage lies in the need for accurate estimation of the machine electrical torque and stator flux linkage. At low speeds, loss of flux control can occur [20]. An additional drawback of the DTC drive is a greater torque ripple stemming from the low switching frequency.

Both drive types rely on knowledge of the machine parameters for control and observation; therefore, initial commissioning is usually required by both the FOC and DTC drives before start-up. The goal of the commissioning stage is to use low-level excitation to obtain estimates of the machine parameters. After the commissioning stage, and during normal operation, online parameter estimation is typically employed.

References

1. V. Del Toro, *Basic Electric Machines,* Prentice-Hall, Englewood Cliffs, NJ, 1990.
2. G. K. Dubey, *Power Semiconductor Controlled Drives,* Prentice-Hall, Englewood Cliffs, NJ, 1989.
3. P. C. Krause, O. Wasynczuk, and S. D. Sudhoff, *Analysis of Electric Machinery,* IEEE Press, New York, 1995.
4. D. W. Novotny and T. A. Lipo, *Vector Control and Dynamics of AC Drives,* Oxford University Press, New York, 1996.
5. P. Vas, *Sensorless Vector and Direct Torque Control,* Oxford University Press, New York, 1998.
6. T. Lipo, Recent progress in the development of solid-state AC motor drives, *IEEE Trans. Power Electron.,* 3(2), 105–117, April 1988.
7. W. Leonhard, Adjustable-speed AC drives, *Proc. IEEE,* 76(4), 455–471, April 1988.
8. G. O. Garcia, R. M. Stephan, and E. H. Watanabe, Comparing the indirect field-oriented control with a scalar method, *IEEE Trans. Ind. Appl.,* 41(2), 201–207, April 1994.
9. R. H. Park, Two-reaction theory of synchronous machines: generalized method of analysis-part I, *AIEE Trans.,* 48, 716–730, 1929.
10. H. C. Stanley, An analysis of the induction machine, *AIEE Trans.,* 57, 751–755, 1938.
11. N. P. Rubin, R. G. Harley, and G. Diana, Evaluation of various slip estimation techniques for an induction machine operating under field-oriented control conditions, *IEEE Trans. Ind. Appl.,* 28(6), 1367–1375, December 1992.
12. W. Leonhard, *Control of Electrical Drives,* Springer-Verlag, New York, 1996.
13. J. C. Moreira and T. A. Lipo, A new method for rotor time constant tuning in indirect field oriented control, in *Power Electronics Spec. Conf.,* 573–580, 1990.
14. D. M. Brod and D. W. Novotny, Current control of VSI-PWM inverters, *IEEE Trans. Ind. Appl.,* IA-21(4), 562–570, 1985.
15. P. Tiitinen, P. Pohjalainen, and J. Lalu, The next generation motor control method: direct torque control, DTC, in *Proc. EPE Chapter Symp. Electric Drive Design Appl.,* 1–7, October 1994.
16. M. Depenbrock, Direct self-control (DSC) of inverter fed induction machine, *IEEE Trans. Power Electron,* 3(4), 420–429, 1988.
17. J. Kang and S. Sul, New direct torque control of induction motor for minimum torque ripple and constant switching frequency, *IEEE Trans. Ind. Appl.,* 35(5), 1076–1081, 1999.

18. J. N. Nash, Direct torque control, induction motor vector control without an encoder, *IEEE Trans. Ind. Appl.,* 33(2), 333–341, 1997.
19. T. G. Habetler, F. Profumo, M. Pastorelli, and L. M. Tolbert, Direct torque control of induction machines using space vector modulation, *IEEE Trans. Ind. Appl.,* 28(5), 1045–1053, 1992.
20. D. Telford, M. W. Dunnigan, and B. W. Williams, A comparison of vector control and direct torque control of an induction machine, in *Power Electronics Spec. Conf.,* 1, 421–426, 2000.